ANALYSIS OF STRESS RELAXATION DURING COMPRESSION OF 3D-PRINTED SAMPLES USING MEX TECHNOLOGY AND THE TAGUCHI METHOD

Paweł SZCZYGIEŁ*, Wiktor SZOT*, Natalia KOWALSKA*, Mateusz RUDNIK*

*Faculty of Mechatronics and Mechanical Engineering, Kielce University of Technology, Tysiąclecia Państwa Polskiego 7 Ave., 25-314 Kielce, Poland

pszczygiel@tu.kielce.pl, wszot@tu.kielce.pl, nkowalska@tu.kielce.pl, mrudnik@tu.kielce.pl

received 26 February 2025, revised 29 September 2025, accepted 05 October 2025

Abstract: The study investigated the impact of various Additive Manufacturing parameters in Material Extrusion technology on stress relaxation during compression using a biocompatible filament. The Taguchi method was applied for the analysis. The examined parameters included layer height, shell count (number of contours), nozzle temperature, print orientation, and overlap. The results enabled the assessment of how printing parameters influence elastic moduli and dynamic viscosity coefficients. It was determined that layer height and shell count have the most significant effect on the percentage decrease in stress over time.

Key words: Additive Manufacturing, stress relaxation, compression

1. INTRODUCTION

Additive Manufacturing (AM), as one of the pillars of the Industrial Revolution 4.0, is used to produce usable components in industries such as medicine, automotive, military, rail or aerospace [1, 2]. In addition, there is a dynamic development of Additive Manufacturing in terms of 3D printers and materials used for AM [3, 4]. Therefore, research should be conducted into the mechanical properties, including rheological properties, of components manufactured using Additive Manufacturing technologies.

Stress relaxation in polymeric materials is an important phenomenon that has significance in materials engineering, industry and medicine [5–7]. This phenomenon refers to the gradual reduction of internal stresses under the influence of a given strain [8, 9]. Rheological models can be used to describe stress relaxation curves [9–12]. The model most commonly used is the Maxwell-Wiechert model, which describes a visco-elastic body [11, 13–16].

In Paper [17], the authors investigated the stress relaxation of 3D printed PLA material. A quasi-static tensile test of additively manufactured samples was performed, taking into account the influence of printing parameters such as print orientation and outer wall thickness. The effect of two thermal conditioning treatments on the material's tensile properties was also investigated. Based on the results, the authors found that samples printed in the 0°, 45° directions and having an outer wall were about 17% higher in tensile strength than samples similarly printed but without an outer wall. For stress relaxation, a stress distribution in the range of 11% - 14% was obtained. Maxwell's equation, the standard linear model and Findley's law were used to describe the relaxation. Of the methods described, Findley's law was found to be suitable for predicting the PLA tested. The 0° samples subjected to thermal conditioning treatments degraded the quasi-static and long-term properties of the material.

The authors of paper [11] investigated the stress relaxation and creep of Alumide material produced by selective powder sintering technology. The test samples were fabricated in three print orientations (X, Y, Z) and subjected to compressive stresses. The Maxwell-Wiechert and Kelvin-Voight models were used to describe stress relaxation and creep, respectively. The results showed that there were no clear differences in stress relaxation and creep deformation between the three types of samples. The building direction influences the dynamic viscosity in the stress relaxation and creep tests. The Maxwell-Wiechert and Kelvin-Voight models were found to be fully adequate to describe the experimental curves.

In the case of polymers, the study of stress relaxation phenomena is particularly important because it depends on the polymer's molecular structure and viscoelastic properties [5, 6, 9].

Optimisation of the manufacturing process of 3D printed components is very important [18–20] . This is because changing the value of one of the Additive Manufacturing parameters, e.g.: layer height or fill type, affects the mechanical properties of the printed component, as confirmed in articles [21–29] .

In Paper [19], the authors used the Taguchi method to optimise the melt deposition manufacturing process and determine the influence of Additive Manufacturing technological parameters such as layer height, orientation, printing temperature, air gap and nozzle material on the mechanical properties of the printed composites. The composites are PLA with appropriately weighted carbon fibres. Layer height and nozzle material, according to the results of the study, had the greatest impact on mechanical properties.

The development of Additive Manufacturing has led to its increasing use in medicine [30, 31]. Additive Manufacturing is used to create: medicines, pharmaceuticals, bones, cartilage, tissues, organs, prostheses, orthoses, and visualisation or educational models [30–33]. Such a high use of Additive Manufacturing in medicine is due to the possibility of customised manufacture of e.g. a prosthesis, orthoses or bones [33–35]. Also, in some cases, the fast turnaround time and cost reduction of manufacturing a medical component [30, 33].

In paper [34], the author applied Industry 4.0 conventions to the

DOI 10.2478/ama-2025-0067

design and manufacturing process of polymer models of mandibular anatomical structures. A process consisting of: reconstructive engineering, computer-aided systems, and at-port manufacturing methods was automated. This has reduced the preparation of the surgical template, reduced manufacturing costs and increased the accuracy of the mandible.

In the case of Additive Manufacturing of prostheses or orthoses, it is important, among other things, to maintain dimensional and shape accuracy and to meet high requirements in terms of mechanical properties, including rheological properties [3, 34, 35]. Prostheses or orthoses are subjected to stress during use by patients, so in such cases it is very important to study the rheological properties of these components [14, 31, 33].

Although numerous studies have examined the effects of Additive Manufacturing parameters on the mechanical properties of materials, only a limited number have addressed viscoelastic properties, such as stress relaxation and dynamic viscosity, particularly under compressive loading. Furthermore, the application of the Taguchi method for optimizing these properties in the context of Additive Manufacturing remains scarcely explored.

The aim of this article is to study the influence of selected technological parameters of Additive Manufacturing: layer height, number of contours, nozzle temperature, print orientation, overlap on the viscoelastic properties of the model printed with Material Extrusion technology. Studies of the influence of technological parameters are important for researchers and designers. They make it possible to reject parameters that have no influence or to study the degree of influence. This study is unique because it focuses on viscoelastic properties under compressive conditions and employs the Taguchi method to optimize these properties, an approach that has not been extensively explored previously.

2. MATERIALS AND METHODS

2.1. Material

PLACTIVE material (Copper 3D, Chile) was used to manufacture the samples. Table 1 shows the material properties.

Tab. 1. PLACTIVE properties [36]

Mechanical properties	Value	Test method
Tensile Yield Strength	60 MPa	D882
Tensile Strength at Break	53 MPa	
Tensile Modulus	3.6 GPa	
Tensile Elongation	6 %	
Flexural Strength	83 MPa	D790
Flexural Modulus	3.8 GPa	

PLACTIVE is a high-quality PLA nanocomposite enhanced with a patented Nano-Copper additive, offering over 99.99% antimicrobial effectiveness against bacteria, viruses, and fungi. Clinically tested for prosthetics and ideal for other medical applications, it is biocompatible, skin-safe (ISO 10993 certified), and maintains strong mechanical properties. With ISO 9001/2015 and REACH compliance, it's also thermoformable, biodegradable, and non-toxic [36].

The filament's chemical composition is primarily composed of Polylactide resin (> 99% by weight) with the addition of NanoCu PCZ001 (< 1% by weight) [37].

2.2. Sample preparation

The shape of the test sample is based on ISO 3384-1:2024 - Rubber, vulcanised or thermoplastic - Determination of stress relaxation in compression - Part 1: Testing at constant temperature, shown in the Figure 1.

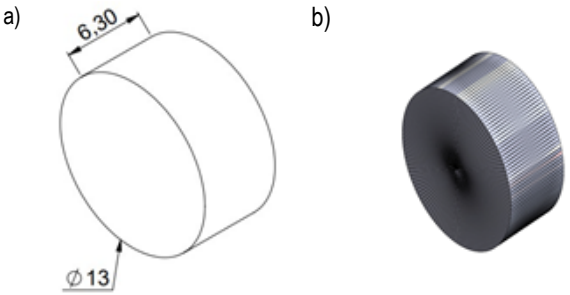

Fig. 1. Sample model: a) dimensions, b) STL view

The samples were designed in SOLIDWORKS software (Dassault Systèmes, Waltham, Massachusetts, USA) and then saved in STL (Standard Triangulation Language) format. The parameters for saving the STL file are: resolution: adjusted; deviation: 0.0016 mm; tolerance 5°. The number of triangles generated as a result of saving the file in STL format: 568. The STL file was then imported into Bambu Studio (Bambu Lab, Shenzhen, China), where the technological parameters were set and the operation of dividing the model into layers was performed.

2.3. Material Extrusion

Material Extrusion (MEX) technology dispenses material through a heated head onto the working platform [38–40]. Filament in the form of a filament fed into a suitably heated nozzle is extruded in semi-liquid form onto the working platform of the 3D printer, making a 3D model layer by layer [40, 41]. The temperature of the nozzle is set depending on the material used for printing [40, 41].
The constant parameters used to print the samples are shown in Table 2.

Tab. 2. Constant technological parameters used in the study

Parameter	Value
Infill density, %	100
Infill pattern	Rectilinear
Speed, mm/s	30
Bed temperature, °C	50

An X1 Carbon printer (Bambu Lab, Shenzhen, China) was used to produce the samples. The printer was equipped with a 0.4 mm print head and a heated PEI textured work table.

Five input factors with three different degrees of variation were selected for the study (Table 3). Shell refers to the number of contours of the model being produced, while overlap is a parameter defining the distance between infill and contour (expressed as a percentage), temperature refers to the temperature of the extruder. Orientation refers to the positioning of the model on the printer build platform during printing (Figure 2).

Tab. 3. Levels of variability of input factors

Parameter		Level		
		1	2	3
A	Layer height, mm	0.1	0.2	0.3
B	Shell	2	9	16
C	Temperature, °C	190	200	210
D	Orientation	X	Y	Z
E	Overlap	15	40	65

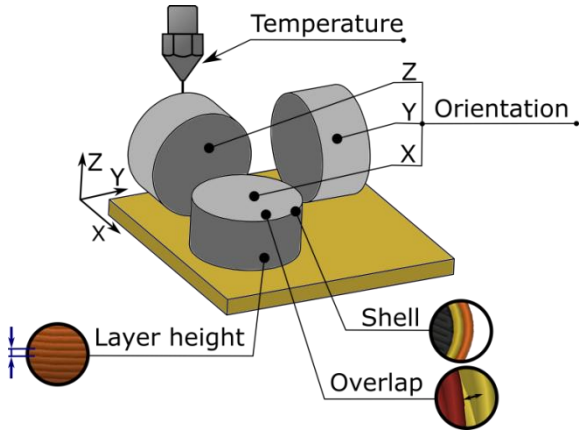

Fig. 2. Characteristics of the input factors

Table 4 shows the L27 orthogonal matrix showing how the input factors were combined. 10 replicates were performed obtaining 27 runs giving a total of 270 samples.

Tab. 4. L27 orthogonal matrix

No.	A	B	C	D	E
1	1	1	1	1	1
2	1	1	2	2	2
3	1	1	3	3	3
4	1	2	1	2	2
5	1	2	2	3	3
6	1	2	3	1	1
7	1	3	1	3	3
8	1	3	2	1	1
9	1	3	3	2	2
10	2	1	1	2	3
11	2	1	2	3	1
12	2	1	3	1	2
13	2	2	1	3	1
14	2	2	2	1	2
15	2	2	3	2	3
16	2	3	1	1	2
17	2	3	2	2	3
18	2	3	3	3	1
19	3	1	1	3	2
20	3	1	2	1	3
21	3	1	3	2	1
22	3	2	1	1	3
23	3	2	2	2	1
24	3	2	3	3	2
25	3	3	1	2	1
26	3	3	2	3	2
27	3	3	3	1	3

2.4. Maxwell-Wiechert model

The five-parameter Maxwell-Wiechert model was used to describe the stress relaxation curves obtained from the stress relaxation tests. Fitting of the rheological model to the experimental curves was carried out using the Lebvenberg-Marquadtaw algorithm in OriginPro software (OriginLab Corporation, One Roundhouse Plaza, Suite 303, Northampton, MA 01060, UNITED STATES).

An equation describing the five-parameter Maxwell-Wiechert model was used, including all parameters of this model (1) [11, 13].

$$\sigma(t) = \varepsilon_0 \left(E_0 + E_1 e^{\frac{-E_1 t}{\mu_1}} + E_2 e^{\frac{-E_2 t}{\mu_2}} \right) \quad (1)$$

where: ε_0 – unit initial strain, %; E_0, E_1, E_2 – elastic moduli, MPa; μ_1, μ_2 – dynamic viscosity coefficients, MPa; t – time, s.

The mechanical analogy of the Maxwell-Wiechert model is shown in Figure 3.

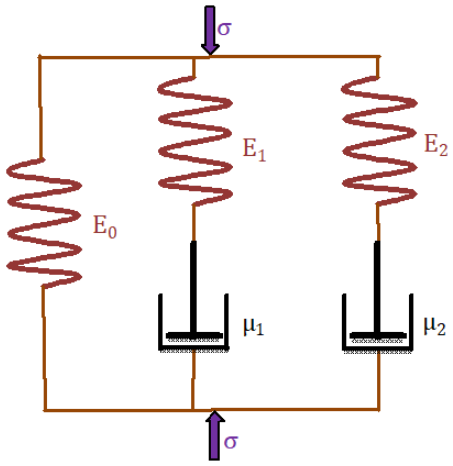

Fig. 3. Mechanical analogy of the five-parameter Maxwell-Wiechert model [14]

The equivalent modulus of E_z was calculated from equation (2) [13]:

$$E_z = E_0 + E_1 + E_2 \quad (2)$$

In addition, the decrease in stress over time was calculated according to equation (3) [14].

$$R_\sigma = \frac{\sigma_0 - \sigma_t}{\sigma_0} \cdot 100\% \quad (3)$$

where: σ_0 – initial stress, MPa; σ_t – stress after time t, MPa.

2.5. Taguchi's Method of Experiment

The research was conducted based on the Taguchi method. In the Taguchi method, the existence of an optimum level of the output factor is assumed. The aim of the investigation is to determine the influence of the individual input factors and the loss function (SN - Signal/Noise ratio) representing the variability of the output factor under study due to process disturbances. Obtaining this information allows optimisation measures to be taken. For each input factor, the value of the loss function at each level of variation is calculated to assess the robustness of the input factors to the effects of disturbances [42]. In order to minimise the values of the loss function, the

DOI 10.2478/ama-2025-0067

SN factor is calculated from the formula (4). This formula applies when the target value of the loss function is 0 ('the smaller the final value the better').

$$SN = -10\,log\left(\frac{1}{n}\sum y_{ij}^2\right) \quad (4)$$

where n – numer of measurements; y – measured output characteristic.

2.6. Method of testing

The test samples were subjected to compressive tension. The appearance of the test rig is shown in the Figure 4. The test parameters set for the stress relaxation tests are as follows: preload F_p =280 N, speed of displacement of the cross-member of the testing machine to obtain the stress v = 10 mm/s, permanent deformation ε_{const} = 0.63 mm, stress relaxation test duration t = 600 s.

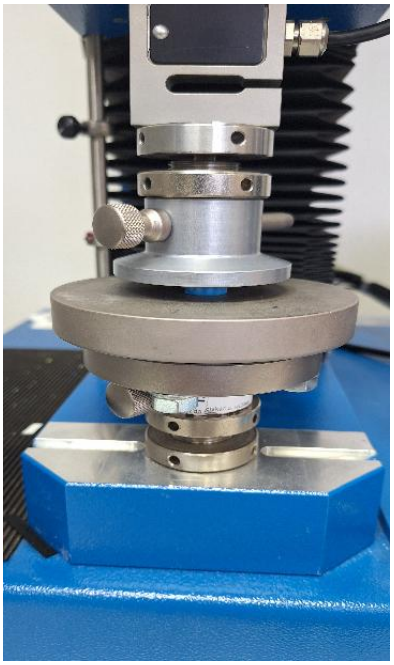

Fig. 4. View of the stress relaxation test

3. RESULTS

The results of the study are divided into two subsections: stress relaxation tests and an analysis of the effect of selected Additive Manufacturing parameters on stress relaxation parameters.

3.1. Stress relaxation tests

The samples shown in Figure 1 were manufactured and subsequently subjected to compressive stresses according to the input factors adopted (Table 3). Examples of stress relaxation curves obtained from the tests for series 1 (Table 4) are shown in Figure 5. The translation of the results shown in Figure 5a is due to the difficulty of realising the unit stroke, which must be performed at the fastest possible speed, which is difficult to achieve under laboratory conditions.

An example fit, of the Maxwell-Wiechert model described by equation (1), is shown in Figure 5b for series 1 and sample 1. The approximations were performed with OriginPro software, which uses the Levenberg-Marquardt algorithm.

As a result of fitting for series 1 and sample 1, parameter values such as σ_0 = 10.2 MPa, σ_1 = 0.1 MPa, σ_2 = 0.1 MPa, t_1 = 11 s, t_2 = 225 s and fitting coefficients χ^2 = 0.000005, R^2 = 0.9959 were obtained for each stress relaxation curve as a result of fitting the Maxwell-Wiechert model. Based on the model parameters obtained, the elastic moduli and dynamic viscosity coefficients were calculated and are shown in Table 5 for the 27 series.

The analysis of the experiment results (Table 5) revealed that the elastic modulus E_0 ranged from 85.7 MPa to 104.8 MPa, with the lowest values observed in experiments 24–27. The moduli E_1 and E_2 were noticeably lower than E_0. The highest values of E_1 and E_2 (above 2 MPa) appeared mainly at lower E_0 values. The dynamic viscosity (μ_1 and μ_2) showed significant variation — μ_1 ranged from 11 to 35 MPa·s, while μ_2 reached values from 188 MPa·s to 703 MPa·s. Experiments 22–27 were characterized by particularly high μ_1 and μ_2 values. A correlation was observed between lower E_0 values and higher E_1, E_2, μ_1, and μ_2 values.

The calculated values of elastic moduli and dynamic viscosity coefficients were used for the Taguchi method.

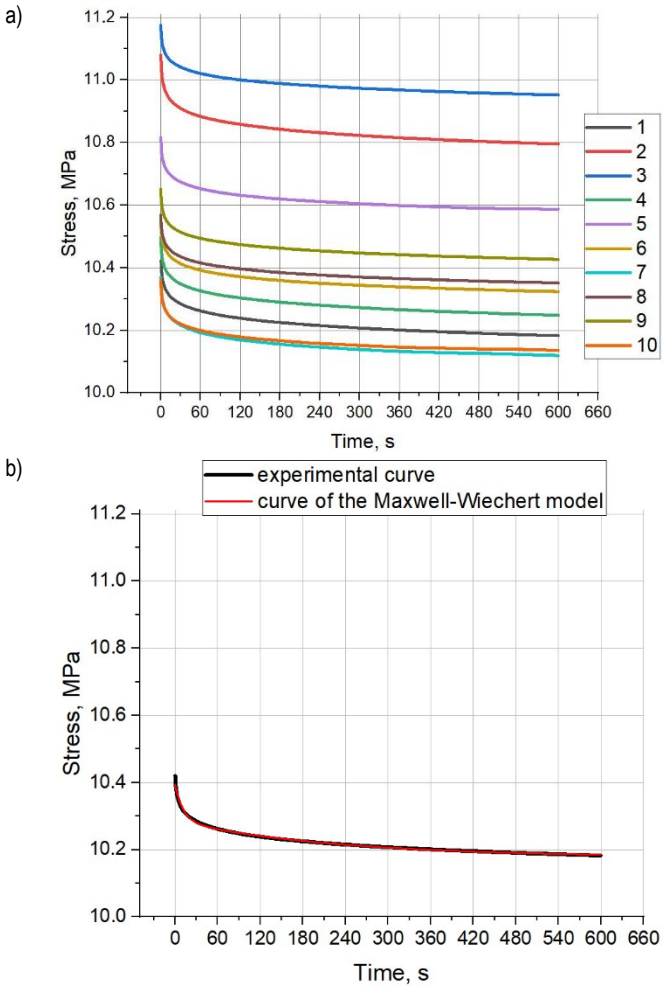

Fig. 5. Stress relaxation tests: a) example of experimental curves, b) example of rheological model fitting

Tab. 5. Modulus of elasticity and dynamic viscosity coefficients in PLA Active material

Number of the experiment	E_0, MPa	E_1, MPa	E_2, MPa	μ_1, MPa · s	μ_2, MPa · s
1	103.3	1.1	1.0	12	215
2	98.3	1.2	1.2	14	260
3	100.7	1.0	0.9	11	188
4	102.9	1.2	1.2	13	261
5	104.2	1.0	1.0	12	266
6	99.9	1.6	1.5	18	328
7	102.5	1.3	1.7	19	476
8	101.5	1.4	1.3	16	301
9	104.7	1.0	1.0	12	266
10	94.3	1.4	1.4	17	340
11	104.8	1.3	1.2	14	236
12	102.6	1.3	1.1	14	201
13	91.7	2.5	2.3	27	458
14	102.0	1.4	1.2	15	222
15	101.4	1.5	1.3	17	264
16	102.4	1.3	1.1	14	207
17	98.3	1.7	1.6	20	341
18	100.2	1.5	1.4	18	332
19	102.9	1.3	1.2	15	275
20	91.3	2.4	2.1	25	434
21	101.0	1.8	1.6	20	317
22	95.7	2.4	2.8	34	703
23	92.5	2.6	2.5	35	586
24	89.5	2.7	2.7	35	608
25	89.8	2.7	2.4	29	510
26	85.7	2.4	2.5	30	565
27	85.7	2.4	2.5	30	565

Table 6 shows the influence of input factors on the values characterising the Maxwell-Wiechert model. The values presented in the table were obtained as the arithmetic mean value of the average values obtained for the series at a given level of variation of a given input factor.

Analysis of the influence of the input factors (A-E) and their three levels of variation on the parameters of the Maxwell-Wiechert model showed that factors A and B had the greatest influence on the elastic moduli and dynamic viscosities. In the case of elastic modulus E_0, the most significant influence was observed for factor A, where the difference between level 1 and level 3 was 9.3 MPa, while the other factors showed more similar values, not exceeding 3.2 MPa. A similar trend was observed for E_1 and E_2 moduli, with factor A showing the greatest variation, reaching a difference of 1.1 MPa, indicating that it plays a key role in shaping the elastic properties of the samples tested.

In the analysis of dynamic viscosity (μ_1 and μ_2), the influence of factor A also dominated, where the difference in values for μ_1 was as much as 14.1 MPa·s (from 14.1 MPa·s at level 1 to 28.2 MPa·s at level 3). For μ_2, factor A showed even greater significance, with a range of values from 284.5 MPa·s to 506.9 MPa·s - a difference of as much as 222.4 MPa·s. Factor B also had a significant effect on μ_2, with a difference between levels of 136.7 MPa·s. The other factors (C, D, E) had a more equal effect on both elasticity and dynamic viscosity moduli, showing less variation between levels of variation, suggesting their limited role in the stress relaxation process.

In summary, the analysis showed that factors A and B had a dominant effect on the parameters of the Maxwell-Wiechert model, particularly in terms of dynamic viscosity μ_1 and μ_2 and elastic moduli E_1 and E_2, while factors C, D and E had a smaller, more balanced effect.

Tab. 6. Influence of input factors and their levels of variation on the parameters characterising the Maxwell-Wiechert model

Par.	Unit	Level	A	B	C	D	E
E_0	MPa	1	102.0	99.9	98.4	98.2	98.3
		2	99.7	97.7	97.6	98.1	99.0
		3	92.7	96.7	98.4	98.0	97.1
E_1	MPa	1	1.2	1.4	1.7	1.7	1.8
		2	1.6	1.9	1.7	1.7	1.5
		3	2.3	1.8	1.6	1.7	1.7
E_2	MPa	1	1.2	1.3	1.7	1.6	1.7
		2	1.4	1.8	1.6	1.6	1.5
		3	2.3	1.7	1.6	1.7	1.7
μ_1	MPa·s	1	14.1	15.8	20.2	19.9	21.0
		2	17.4	23.0	20.0	19.6	18.0
		3	28.2	20.9	19.4	20.2	20.6
μ_2	MPa·s	1	284.5	273.9	382.8	352.9	364.7
		2	288.9	410.6	356.5	349.3	318.2
		3	506.9	395.8	341.0	378.1	397.4

3.2. Taguchi analysis

Based on the compressive stress relaxation tests, the mean percentage decreases in stress over time were calculated using equation (3), the results are shown in Figure 6 with the standard deviation values highlighted.

It can be seen that the smallest decreases in stress over time were recorded for samples made at a lower layer height.

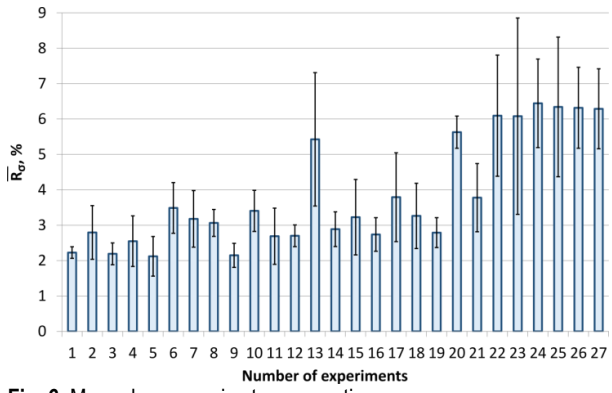

Fig. 6. Mean decreases in stress over time

DOI 10.2478/ama-2025-0067

The smallest decreases (around 2 %) were observed for series 1, 3, 5, 9, where the standard deviation values took values in the range of 0.2 - 0.6 %. The largest average percentage decreases in stress were observed for series numbers 20, 22-27, where values in the range of 5.6 - 6.4 % were obtained, with a standard deviation of 0.5 - 2.8 %. It is worth noting that a common parameter for these combinations is the layer height of 0.3 mm. The exception is series number 13 for which the input factors with values of: A = 0.2 mm, B = 9; C = 190 °C, D = position Z and E = 15 % resulted in a significant decrease in stress averaging 5.4 %, with a standard deviation of 1.9 %.

The Figure 7 shows the interference resistance of the input factors. Formula (4) was used to calculate the SN value. It can be seen that the Layer height and Shell parameters are the least resistant to interference and should therefore be focused on in order to optimise the manufacturing process.

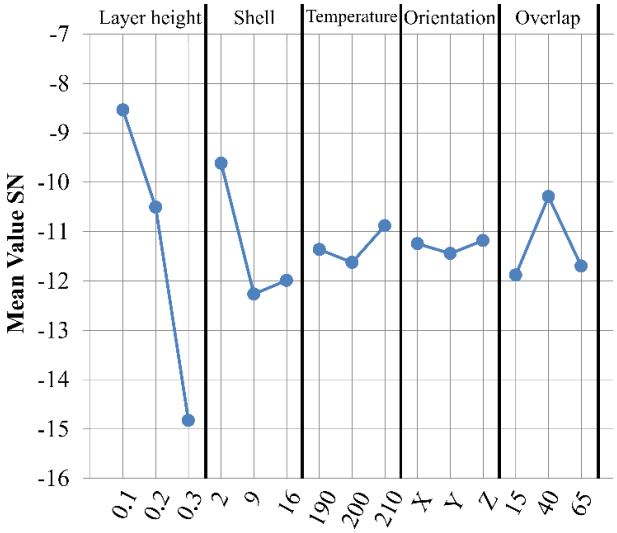

Fig. 7. Taguchi results of signal-to-noise (S/N) response graph

Table 7 shows the percentage effect of individual input factors on the compressive stress drop. As before, the values presented in the table were obtained as the arithmetic mean of the average values obtained for the series at a given level of variation of a given input factor.

Analysis of the influence of the input factors (A-E) and their three levels of variation on the percentage decrease in stress over time showed that factors A and B had the greatest influence.

Factor A had the most variation between levels, with the percentage decrease in stress increasing from 2.64% at level 1, through 3.35% at level 2, to 5.53% at level 3 - the difference between the extreme levels was 2.89%, demonstrating the significant influence of this factor.

Factor B also showed a noticeable impact, with values of 3.13% (level 1), 4.26% (level 2) and 4.13% (level 3). The difference between level 1 and level 2 reached 1.13%, suggesting that the variation in this parameter was significant for the stress relaxation analysis.

For factors C, D and E, the impact was much more balanced. For factor C, the stress relaxation percentages varied slightly between 3.73% and 3.93%, giving a difference of 0.20%. Similarly, D showed stable results, ranging from 3.79% to 3.90%, a difference of only 0.11%.

Factor E showed a moderate impact, with a value of 4.04% at level 1, 3.49% at level 2 and 3.99% at level 3. The difference between the extreme levels was 0.55%, showing that its role was greater than factors C and D, but still less than A and B.

In summary, the analysis showed that factors A and B had the greatest influence on the percentage decrease in stress over time, with marked differences between the levels of variation. C, D and E had a more stable effect, with noticeably less influence on stress relaxation. Figure 8 shows a graph illustrating the effect of individual input factors on the percentage decrease in stress over time.

Tab. 7. Influence of input factors and their levels of variation on the percentage decrease in stress over time

Level / Param.	1	2	3
A	2.64	3.35	5.53
B	3.13	4.26	4.13
C	3.86	3.93	3.73
D	3.90	3.79	3.82
E	4.04	3.49	3.99

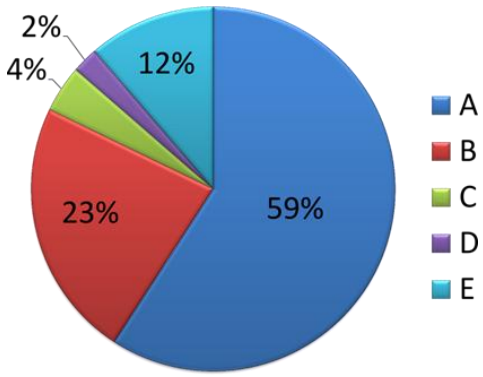

Fig. 8. Effect of input factors on the percentage decrease in stress over time

4. DISCUSSION

The obtained values of the coefficient of determination R^2 for all series were close to 1, while the values of the χ^2 statistic were close to 0. This indicates a strong fit of the five-parameter Maxwell-Wiechert model to the experimental stress relaxation curves. The graphical interpretation (Fig. 5b) further illustrates and confirms the strong fit of the rheological model to the experimental curve, as evidenced by the overlap of the red model line with the black measurement data line.

Similar observations have been reported in the literature, where the five-parameter Maxwell-Wiechert model was used to describe stress relaxation in 3D printed polymer materials [10,11,13,14].

The analysis of the influence of factors (A-E) and their levels of variability on the parameters of the five parameter Maxwell-Wiechert model E_0, E_1, E_2, μ_1, μ_2 and the percentage decrease in stress over time revealed dependencies. They indicate the dominant role of certain technological parameters of 3D printing on the phenomenon of stress relaxation in samples produced using MEX technology.

Among the studied technological parameters of additive manufacturing, the layer height (A) and shell (B) had the greatest

influence. They affected both the elasticity modules E_0, E_1, E_2, and the dynamic viscosity coefficient μ_1, μ_2 of the Maxwell-Wiechert model. The differences between the levels of variability of these parameters were the most significant, which confirms their important role in the stress relaxation process. The other analysed 3D printing parameters, such as nozzle temperature (C), print orientation (D), and overlap (E), showed more balanced values between the levels of variability. Their influence on the stress relaxation process was smaller.

An analysis of the percentage decrease in stress further confirms the above observations. Layer height (A) and shell (B) proved to be the most important factors, with layer height being the dominant factor in terms of its influence on the stress relaxation process. These results indicate that the use of smaller layer heights leads to a slowdown in the relaxation process, which can be associated with better interlayer adhesion. On the other hand, increasing the shell increases the density of the model, which also affects the rheological response of the material.

5. SUMMARY

In the case of stress relaxation phenomena, for all the series studied, the R^2 values were close to 1 and the χ^2 values were close to 0 (indicating a better model fit). The graphical interpretation (Figure 5b) confirms the fit of the Maxwell-Wiechert model for the stress relaxation curves through the agreement of the rheological model curve, which confirms the sufficiency of using the five-parameter model for this purpose.

Based on the analysis of the influence of the input factors (A-E) and their levels of variation on the Maxwell-Wiechert model parameters and the percentage decrease in stress over time, the following conclusions can be drawn:

- Factors A (Layer Height) and B (Shell) showed the strongest influence on both the Maxwell-Wiechert model parameters - in particular the dynamic viscosity μ_1 and μ_2 - and the percentage decrease in stress over time. Their influence was clearly stronger compared to the other factors. The differences between the levels of variation for these parameters were the most significant, confirming their key role in the stress relaxation process;
- Factors C (Nozzle Temperature), D (Print Orientation) and E (Overlap) showed more even values between levels, both for the elasticity and dynamic viscosity parameters and for the stress drop. Their effect on stress relaxation was noticeably smaller, indicating that they do not play a key role in shaping the mechanical properties of the samples tested;
- In the analysis of the percentage decrease in stress over time, factors A and B again showed a significant effect, with Layer Height (A) having the strongest effect, with a difference of as much as 2.89 % between the levels. This confirms that Layer Height significantly affects the rate of stress relaxation, with Contour Number (Shell) also playing an important role, albeit to a lesser extent.
- In order to achieve more favourable mechanical properties for samples printed using MEX technology, particular attention should be paid to the choice of layer height and number of contours. By optimising these parameters, it is possible to control both the elasticity and dynamic viscosity of the material more effectively, as well as to influence the rate of stress drop.

In summary, Layer Height (A) and Shell (B) are the key parameters influencing stress relaxation and Maxwell-Wiechert model parameters, while Nozzle Temperature (C), Print Orientation (D) and Overlap (E) have a more balanced and less significant influence.

This study has some limitations that should be acknowledged. The experiments were conducted using a single type of filament and one AM technology (MEX), which may limit the generalizability of the results to other materials or printing methods. In future work, it is planned to investigate other types of filaments and polymer blends, as well as additional viscoelastic and mechanical properties. Furthermore, alternative statistical optimization methods will be explored, and tests under more realistic manufacturing conditions are intended to better assess the applicability of the findings.

REFERENCES

1. Zmarzły P, Kozior T, Gogolewski D. The effect of non-measured points on the accuracy of the surface topography assessment of elements 3D printed using selected additive technologies. Materials. 2023;16.
2. Ghosh B, Karmakar S. 3D printing technology and future of construction: a review. IOP Conf Ser Earth Environ Sci; 2024.
3. Kroczek K, Turek P, Mazur D, Szczygielski J, Filip D, Brodowski R, et al. Characterisation of selected materials in medical applications; 2022.
4. 4Rwaiha O, Jwaili MA, Rwaiha OM, Ebid E. Novel of 3D printing technology: review. Int J Creative Research Thoughts; 2024.
5. Wang Y, Zhu F, Rao Q, Peng X. A 3D finite strain viscoelastic model with uncoupled structural and stress relaxations for shape memory polymers. Polym Test. 2021;103.
6. Du Y, Wang P, Liang R, Zhou X, Chen S. Automatic testing system for performance parameters of viscoelastic materials. Int J Comput Sci Inf Technol. 2024;3:103–111.
7. Kozior T, Kundera C. Rheological properties of cellular structures manufactured by additive PJM technology. Teh Vjesn. 2021;28: 82–87.
8. Wijesinghe S, Perahia D, Ge T, Salerno KM, Grest GS. Stress relaxation of comb polymer melts. Tribol Lett. 2021;69.
9. Ibrulj J, Dzaferovic E, Obucina M, Kuzman MK. Numerical and experimental investigations of polymer viscoelastic materials obtained by 3D printing. Polymers (Basel). 2021;13.
10. Szot W, Bochnia J, Zmarzły P. Effect of selective laser sintering on stress relaxation in PA12. Polimery. 2024;179–185.
11. Bochnia J, Blasiak S. Stress relaxation and creep of a polymer-aluminum composite produced through selective laser sintering. Polymers (Basel). 2020;12.
12. Lin CY, Chen YC, Lin CH, Chang KV. Constitutive equations for analyzing stress relaxation and creep of viscoelastic materials based on standard linear solid model derived with finite loading rate. Polymers (Basel). 2022;14.
13. Bochnia J. Evaluation of relaxation properties of digital materials obtained by means of PolyJet Matrix technology. Bull Pol Acad Sci Tech Sci. 2018;66:891–897.
14. Bochnia J, Kozior T, Szot W, Rudnik M, Zmarzły P, Gogolewski D, et al. Selected mechanical and rheological properties of medical resin MED610 in PolyJet Matrix three-dimensional printing technology in quality aspects. 3D Print Addit Manuf. 2024;11:299–313.
15. Stankiewicz A, Juściński S. How to make the stress relaxation experiment for polymers more informative. Polymers (Basel). 2023;15.

16. Chepurnenko AS, Kondratieva TN, Al-Wali E. Processing of polymers stress relaxation curves using machine learning methods. 2023.
17. Bertocco A, Bruno M, Armentani E, Esposito L, Perrella M. Stress relaxation behavior of additively manufactured polylactic acid (PLA). Materials. 2022;15.
18. Stepanov DY, Dontsov YV, Panin SV, Buslovich DG, Alexenko VO, Bochkareva SA, et al. Optimization of 3D printing parameters of high viscosity PEEK/30GF composites. Polymers (Basel). 2024;16.
19. Guduru KK, Setti SG. 3D printed carbon fiber reinforced PLA composite using fused deposition modeling by Taguchi's optimization: influence of printing parameters. Int J Interact Des Manuf. 2024.
20. Abed SA, Hassan SR, Jomah AJS, Hanon MM. Prediction on the wear rate of epoxy composites reinforced micro-filler of the natural material residue using Taguchi–neural network. Eureka Phys Eng. 2023;149–159.
21. Zubrzycki J, Quirino E, Staniszewski M, Marchewka M. Influence of 3D printing parameters by FDM method on the mechanical properties of manufactured parts. Adv Sci Technol Res J. 2022;16:52–63.
22. Vochozka V, Černý P, Šramhauser K, Špalek F, Kříž P, Čech J, et al. Fused filament fabrication 3D printing parameters affecting the translucency of polylactic acid parts. Polymers (Basel). 2024;16:2862.
23. Bruère VM, Lion A, Holtmannspötter J, Johlitz M. The influence of printing parameters on the mechanical properties of 3D printed TPU-based elastomers. Prog Addit Manuf. 2023;8:693–701.
24. Alzyod H, Ficzere P. Material-dependent effect of common printing parameters on residual stress and warpage deformation in 3D printing: a comprehensive finite element analysis study. Polymers (Basel). 2023;15.
25. Kowalska N, Szczygieł P, Skrzyniarz M, Błasiak S. Effect of shells number and machining on selected properties of 3D-printed PLA samples. Polimery. 2024;69:186–190.
26. Rudnik M. Study of cellular structures built from self-similar models and repeatable structures manufactured by FDM/FFF technology. Polimery. 2024;173–178.
27. Faidallah RF, Abd-El Nabi AM, Hanon MM, Szakál Z, Oldal I. Compressive and bending properties of 3D-printed wood/PLA composites with re-entrant honeycomb core. Results Eng. 2024;24.
28. Estefanía D, Pérez C, Geovanny E, Novay Z, Patricio H, Mazón C, et al. Elasticity and plasticity of PLA, PETG, ABS polymers for printing automotive parts. Rev Multidiscip Investig Científica. 2024;8:51–66.
29. Grigoriev S, Nikitin N, Yanushevich O, Krikheli N, Khmyrov R, Strunevich D, et al. Experimental and statistical study of strength properties of FDM-printed specimens made from ABS, PLA and PETG plastics depending on the percentage and structure of filling. Research Square. 2024. Available from: https://www.researchsquare.com/article/rs-4627817/v1
30. Yu J. The application and significance of 3D printing technology in biomedicine. Appl Comput Eng. 2024;58:215–221.
31. Mathews Jacob J, Nachiappan B. An overview on 3D printing technology: technological, materials, and applications; 2023.
32. Wang Z, Wang XY, Yu X. Application of 3D printing surgical training models in the preoperative assessment of robot-assisted partial nephrectomy. BMC Surg. 2024;24.
33. Ali F, Kalva SN, Koc M. Advancements in 3D printing techniques for biomedical applications: a comprehensive review of materials consideration, post processing, applications, and challenges. 2024.
34. Turek P. Automating the process of designing and manufacturing polymeric models of anatomical structures of mandible with Industry 4.0 convention. Polimery. 2019;64:522–529.
35. Zakręcki A, Cieślik J, Bazan A, Turek P. Innovative approaches to 3D printing of PA12 forearm orthoses: a comprehensive analysis of mechanical properties and production efficiency. Materials. 2024;17.
36. Cooper3D. Material technical datasheet PLACTIVE; 2025.
37. Cooper3D. Material safety data sheet PLACTIVE; 2025.
38. Karimi A, Rahmatabadi D, Baghani M. Various FDM mechanisms used in the fabrication of continuous-fiber reinforced composites: a review; 2024.
39. Ma T, Zhang Y, Ruan K, Guo H, He M, Shi X, et al. Advances in 3D printing for polymer composites: a review; 2024.
40. Bustos Seibert M, Mazzei Capote GA, Gruber M, Volk W, Osswald TA. Manufacturing of a PET filament from recycled material for material extrusion (MEX). Recycling. 2022;7.
41. Mittal YG, Patil Y, Kamble PP, Gote GD, Mehta AK, Karunakaran KP. Warpage control in thermoplastic ABS parts produced through material extrusion (MEX)-based fused deposition modeling (FDM). Rapid Prototyp J. 2024;30:1822–1835.
42. Shina S. Industrial design of experiments. Cham: Springer International Publishing; 2022.

Paweł Szczygieł: https://orcid.org/0000-0002-3113-3557
Wiktor Szot: https://orcid.org/0000-0001-9512-9680
Natalia Kowalska: https://orcid.org/0000-0003-3043-7812
Mateusz Rudnik: https://orcid.org/0000-0001-5096-608X